Observation of growth-mode change under a magnetic field in $YBa_2Cu_3O_{7-x}$

Yanwei Ma, Kazuo Watanabe, Satoshi Awaji, and Mitsuhiro Motokawa
Institute for Materials Research, Tohoku University, Sendai 980-8577, Japan
and CREST, Japan Science and Technology Corporation, Tsukuba 305-0047, Japan
(Received 21 February 2001; revised manuscript received 16 July 2001; published 6 May 2002)

$YBa_2Cu_3O_{7-x}$ (YBCO) films were grown on metallic substrates by a metalorganic chemical vapor deposition process in high magnetic fields. We used a combination of scanning electron microscopy (SEM), atomic force microscopy (AFM), x-ray diffraction, and transport-property measurements. By imaging the as-grown surfaces of YBCO films with high-resolution SEM and AFM, we have directly observed the growth-mode change from the spiral growth mode at zero field to the two-dimensional or (3D) island growth mode under an external magnetic field. The surface structures observed provide insight into the mechanism of crystal growth operative during the formation of YBCO films grown using the our field-assisted chemical vapor deposition technique. The possible mechanism of the film growth under the influence of a magnetic field is also analyzed.

DOI: 10.1103/PhysRevB.65.174528 PACS number(s): 74.72.Bk, 74.76.Bz, 74.80.Bj

INTRODUCTION

Since the discovery of high-temperature superconductors (HTS's) in 1986, significant progress has been made towards fabricating long, flexible HTS wires and cables with high transport critical current densities (J_c) for various electrical industry applications. One of the most successful approaches is the oxide powder-in-tube (OPIT) process to produce high-quality silver-sheathed Bi-2212 and Bi-2223 tapes.[1,2] Although thousands of meters of OPIT Bi-based tapes have been fabricated, the intrinsic properties of Bi-based materials, i.e., the temperature dependence of the irreversibility field, appear to limit them to applications at lower temperature (<40 K) or in low fields at higher temperature. Compared to Bi-based superconductors, $YBa_2Cu_3O_{7-x}$ (YBCO) will enable applications at 77 K and in magnetic fields over 1 T. However, high J_c values can only be obtained for YBCO films that are oriented with a high degree of crystalline texture both normal to and within the basal plane. New production methods to realize highly textured YBCO films on metallic tapes are necessary for HTS applications. Recently, several novel approaches based on vapor deposition technologies very different from OPIT, known as the ion-beam-assisted deposition (IBAD) and rolling-assisted biaxially textured substrate (RABiTS) processes,[3,4] have been developed to make YBCO films on metallic substrates by which high J_c values greater than 10^6 A/cm^2 were already demonstrated for short length samples. A key issue in the above approaches is the necessity to use buffer layers, whose function mainly is to prevent diffusion of metal elements into the superconductor during high-temperature processing and also transfers the biaxial texture of the metal substrate to the HTS coating.[5] More recently, significant progress towards a scalable low-cost buffer layer has made at Oak Ridge National Laboratory, which is a major step for achieving an economically and technically viable wire process.[6]

As another approach, the direct deposition of YBCO films on metallic substrates without any buffer layer, is one of the most promising methods for preparing a low-cost superconducting tape.[7] However, lower transport properties in YBCO films directly grown on metallic substrates are the principal limitation to technological applications. This limitation is strongly correlated to the misorientation between the grains. Hence, in order to minimize grain-boundary weak links, a high degree of texture must be obtained. One possible method to produce superconductor grain alignment is to fabricate samples under a high magnetic field.[8,9] The driving force for grain alignment is provided by the anisotropy paramagnetic susceptibility exhibited by the superconductor grains. When placed in a magnetic field, a superconductor grain minimizes its magnetic energy by aligning its axis of maximum paramagnetic susceptibility parallel to the magnetic field.

On the other hand, metalorganic chemical vapor deposition (CVD) technique is considered to be a very promising method because of its advantages of a high growth rate, conformal coverage, and its ability to coat complex shapes. YBCO films with high J_c more than 10^6 A/cm^2 at 77 K were easily fabricated on single-crystal substrates by this method.[10] In addition, for practical YBCO superconductors as a long wire or tape in electric power applications, cheap, robust, and flexible metallic substrates are required.

If the magnetic field is applied during a film fabrication process, the orientation of grains and other field effects for film growth are expected. Our study is motivated by this idea with the aim of improving the superconducting properties of YBCO films grown on metallic substrates through combining the magnetic grain alignment and CVD techniques. In order to optimize the processing of HTS films under a magnetic field, it is important to understand the growth mechanism on a technically interesting substrate. Since this may allow better control of the film's microstructure and thus its properties. In this work we will show that for YBCO films on polycrystalline silver substrates, the surface morphology drastically changes with increasing the magnetic field. In addition, we address the discovery of new phenomena relevant to the growth mode change in YBCO films induced by an external magnetic field.

EXPERIMENTAL PROCEDURE

YBCO films were grown on polycrystalline silver substrates by metalorganic chemical vapor deposition

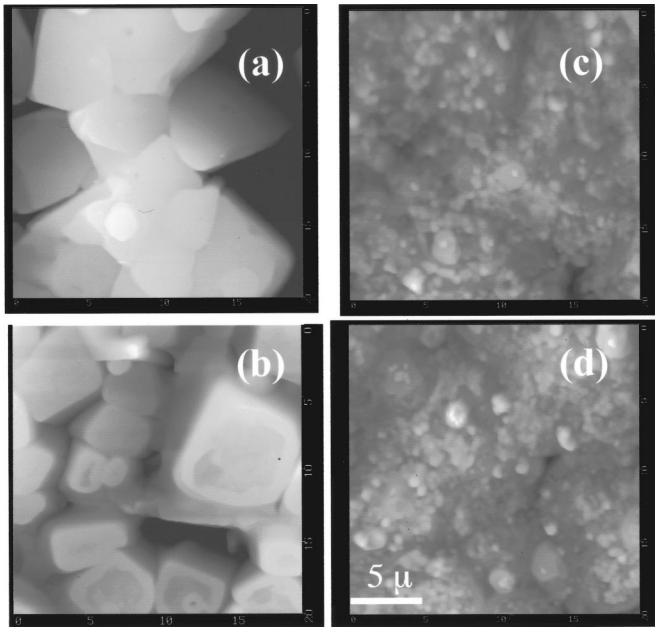

FIG. 1. AFM images of YBCO films grown at different magnetic fields. The scan size is 20 μm$\times$20 μm. (a) 0 T, (b) 2 T, (c) 4 T, and (d) 8 T.

(MOCVD) in high magnetic fields. Polycrystalline silver substrates, approximately $10\times5\times0.2\,\mathrm{mm}^3$ in size, were used; they were mechanically polished prior to deposition. The substrates were set in a vertical reactor, which was installed in the room-temperature bore of a cryogen-free superconducting magnet,[11] and the film deposition was carried out at a constant vertical magnetic field of 0, 2, 4, 6, and 8 T. To be concise, hereinafter we refer to the magnetic field during deposition by H_{CVD}. Nonaligned films were fabricated employing identical conditions in the absence of a magnetic field. The deposition conditions were the same as previously published.[12] The films were slowly cooled to room temperature from the deposition temperature (850 °C) in 1 atm of oxygen. The transport J_c at 77 K and its magnetic field dependence were evaluated by a standard four-probe technique with a criterion of 0.5 μV/cm. YBCO films were characterized by x-ray diffraction (XRD). The surface morphology of YBCO films was investigated by scanning electron microscopy (SEM) and atomic force microscopy (AFM).

RESULTS

Figure 1 shows the AFM images for the films deposited at different magnetic fields. In the case of the absence of a magnetic field, the films exhibit large rectangular grains, and large voids and poor interconnection are present. At 2 T, the grain shape seems similar to that of the 0 T films, but the grain size is reduced. Under a field of above 2 T, the crystallites of films were more homogeneous and irregular grains $\sim$1–2 μm were well connected to each other, compared with that without the magnetic field. Clearly, the intergrain connectivity and morphology were less influenced by fields over 4 T. Thus, with increasing magnetic field, the grain size was reduced, but the grain connectivity was improved. In addition, we have already confirmed that the crystallinity of YBCO films was improved by applying a magnetic field during the CVD deposition,[13] which is attributed to the magnetic field orientation effect.

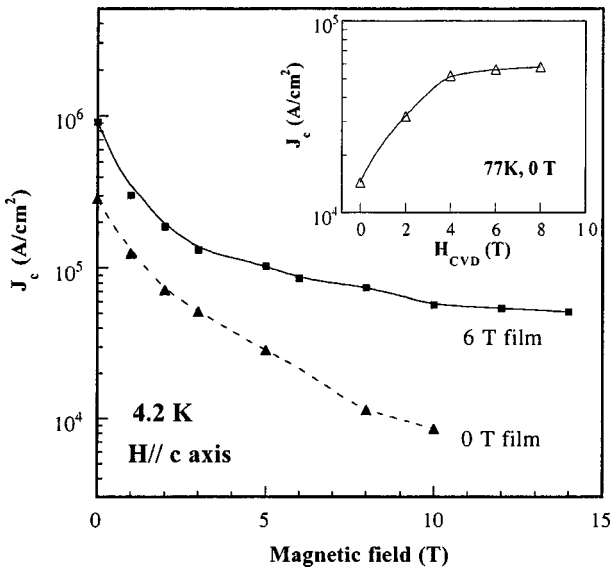

FIG. 2. Magnetic field dependence of the transport current density at 4.2 K, $H\|c$, for films deposited under $H_{\mathrm{CVD}}=0$ and 6 T. The inset shows the J_c values at 77 K, zero field, as a function of the deposition field H_{CVD}.

Since both the crystallinity and intergrain connections have been improved, the enhancement of critical current densities of YBCO films is also expected. Figure 2 shows the field dependence of transport critical current densities for films deposited under a 0 and 6 T magnetic field at 4.2 K. Notice that there is a strong increase in J_c for the films deposited under a magnetic field. Clearly, for field samples, J_c values also exhibited much less of the field dependence behavior, implying that field films have strong flux pinning with increasing magnetic field. This behavior is similar to the field dependence at 77 K.[13] Shown in the inset of Fig. 2 is the self-field values of J_c at 77 K as a function of the deposition field H_{CVD}. In this plot, J_c increases with increasing the magnetic field up to 4 T and further increasing the magnetic field hardly affects the J_c improvement. Therefore, the above data clearly indicate that the magnetic field is responsible for improving the superconducting properties of YBCO films.

In order to get more information about the microstructures of films deposited with and without the magnetic field, SEM was performed, as shown in Fig. 3. From this figure, it is clear that the structure development with magnetic fields is consistent with the AFM observation (Fig. 1). Furthermore, the most prominent feature for the 0 T film is the presence of growth spirals and steps due to screw dislocations. Growth spirals emanating from both left- and right-handed screw dislocations are clearly seen (indicated by arrows). On the contrary, as for the films deposited in the magnetic fields, no indication for spiral growth features are found. Hence our observations clearly demonstrate that the growth mechanism for the films with and without the field should be different.

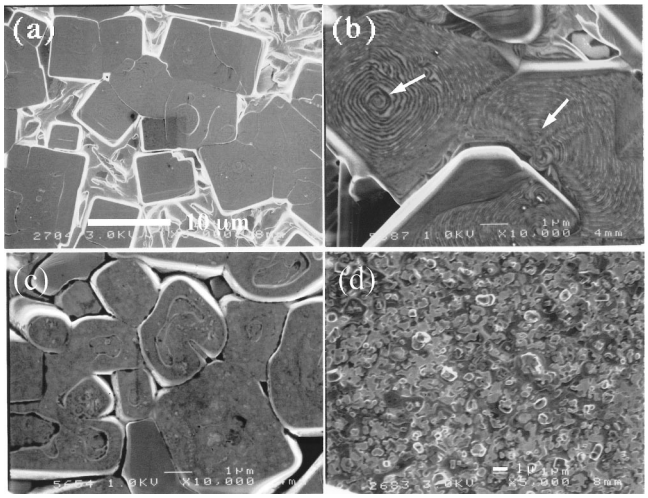

FIG. 3. SEM images of YBCO films grown at different magnetic fields: (a) 0 T, (b) a magnified view for the 0 T film shows the spiral growth mode is preferred in the case of the absence of the magnetic field, (c) high-resolution view for the 2 T film, and (d) high-resolution view for the 4 T film.

The detailed structure of a growth mode becomes visible by atomic force microscopy at high magnification. As expected, the difference in the growth modes between the three films is evident. In the 0 T film, the characteristic spiral growth pattern is clearly present in Figs. 4(a) and 4(b). Not only a large single growth spiral, but also partially connected spiral islands can be observed. The screw dislocations appear to be randomly distributed. The steps between terraces of the growth spirals in AFM images are one unit cell high ($\sim$ 1.2 nm), which indicates that these dislocations have a Burgers vector with a screw component normal to the surface of *c* [001].[14] These observations are in agreement with previous findings that screw dislocations are a general feature of the growth of *c*-axis YBCO films.[14] However, the AFM images of the films grown in magnetic fields are very different from growth in a zero field. The YBCO film growth at 2 T exhibits the two-dimensional (2D) growth behavior: rectangular grains, straight-cut grain edge. In most cases, spaced steps with $\sim$92 nm are observed at the edge of the grain; in particular, no growth spirals are found on the film surface. It has been reported that for the Ag/Au-doped YBCO film grown by pulsed laser deposition, the film consists of well-aligned rectangle-shaped grains, but no any spirals, having a high J_c of $4-8\times10^6$ A/cm^2 (0 T, 77 K).[15] Subsequently, direct evidence of 2D nucleation and growth in laser-ablated YBCO films was also observed.[16] These results support the findings in this study. For the films deposited in magnetic fields above 2 T similarly, no evidence for spiral growth is seen [Fig. 4(d)]. Although they are formed through isolated island growth, it is apparently different from the 2 T case. If it was a 2D island, two-dimensional steps should appear around each hill-like bump. However, no steps around the bump were observed on the above 2 T films, indicating that the film growth was the 3D island mode. Thus it is clear that the spiral growth mode is preferred in the case of the absence of the magnetic field, while the other growth mechanism is possible for YBCO films in the presence of a magnetic field. In other words, the surface morphology change was accompanied by the growth-mode change.

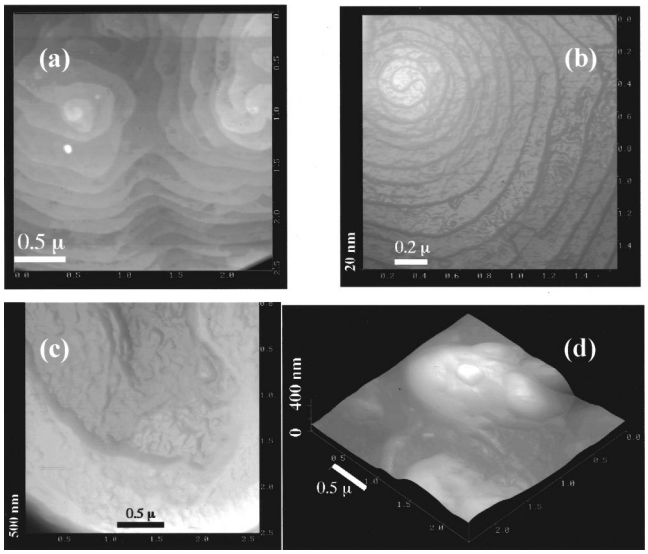

FIG. 4. High-resolution AFM images of the three films grown at different magnetic fields: (a) 0 T. Connected growth spirals are clearly seen. (b) 0 T. A single-core spiral can often be observed. (c) 2 T, exhibiting 2D-growth behavior. (d) 4 T, exhibiting the 3D-growth mode.

DISCUSSION

It is well known that high-T_c superconductors—e.g., for YBCO—always exhibit an anisotropic paramagnetic susceptibility arising from the conducting Cu-O planes: namely, $\chi_c > \chi_{a,b}$ where χ_c is the paramagnetic susceptibility along the *c* direction and χ_{ab} is the paramagnetic susceptibility normal to the *a*-*b* plane. Hence, when placed in a magnetic field, the magnetic energy is minimized when the axis of maximum susceptibility is parallel to the magnetic field.[8,9] Let us assume homogeneous nucleation and see how the magnetic field plays an important role in the nucleation stage. For simplicity, considering the formation of a 3D nucleus with radius *r*, the Gibbs free energy $G(r)$ can be written as

$$\Delta G(r) = -V_S \Delta G_V + A_{SV}\gamma_{SV} - V_S \Delta G_M, \qquad (1)$$

where V_S is the volume of the nucleus and $\Delta G_V \approx k_B T\sigma$ is the change in free energy for a nucleus formed at a supersaturation σ. Here A_{SV} is the nucleus/vapor phase interfacial area, γ_{SV} the interfacial energy per unit area of interface, and ΔG_M the Zeeman energy of the nucleus.

The extra driving force ΔG_M due to the presence of a magnetic field is a result of the difference in magnitization between the vapor phase and the crystal. This energy can be expressed by

$$\Delta G_M = 1/2 \Delta M_T H, \qquad (2)$$

where ΔM_T is the difference in magnetic moment between the vapor phase and the nucleus at a temperature *T*, and *H* is

the applied magnetic field. In the vapor phase, the magnetic moment per unit volume M_V is given by $\chi_V H$, where χ_V is the paramagnetic susceptibility. In the case the anisotropic nucleus formed in the magnetic field H, the magnetic field moment of the nucleus per unit volume can be written as

$$M_s = -(\chi_c H \cos^2\theta + \chi_{ab} H \sin^2\theta), \tag{3}$$

where θ is the angle between the field H and the direction of the greatest susceptibility the c axis of the nucleus.

Substituting Eqs. (2) and (3) into Eq. (1), the total change in free energy is as follows:

$$\Delta G(r) = -V_S \Delta G_V + A_{SV}\gamma_{SV} - \tfrac{1}{2} V_S H[(\chi_c H \cos^2\theta + \chi_{ab} H \sin^2\theta) - \chi_v H]. \tag{4}$$

The critical radius r^* at which a 3D nucleus becomes stable is determined by the condition $dG/dr = 0$, resulting in

$$r^* = \frac{2\gamma_{SV}}{\Delta G_V + \frac{1}{2}H^2[(\chi_c \cos^2\theta + \chi_{ab}\sin^2\theta) - \chi_v]}. \tag{5}$$

In the case where the magnetic field H is parallel to the nucleus c axis—namely, $\theta = 0$—we obtain

$$r^* = \frac{2\gamma_{SV}}{\Delta G_V + \frac{1}{2}H^2(\chi_c - \chi_v)}. \tag{6}$$

One can note that $\chi_V < \chi_c$.[9] Thus, we may estimate the critical energy barrier for nucleation by substituting Eq. (6) into Eq. (4) from

$$\Delta G^*_{H\|c} = \frac{16\pi\gamma^3_{SV}}{3[\Delta G_V + \frac{1}{2}H^2(\chi_c - \chi_v)]^2}. \tag{7}$$

Clearly, not only the barrier for nucleation becomes lower, but also the size of critical radius is reduced when the magnetic field is applied. It is recognized that the smaller the radius, the more stable the nucleus grows. Hence the probability to nucleate islands on the silver substrate surface is enhanced. In other words, there is a greater tendency for nuclei that are aligned with the c axis parallel to the field to take place. Such a phenomenon is easily understood as a consequence of the above-described effect of the magnetic field of lowering the energy barrier for nucleation. Thus the incoming adatoms would form their own nuclei by themselves because of the short diffusion length of particles and suppressed mobility (as shown in Fig. 1, the magnetic field dramatically reduces the grain size of YBCO, suggesting that the surface mobility and diffusion length for arriving adatoms might be suppressed by the presence of a magnetic field), and the areal density of nuclei on the film surface should effectively increase with the strength of a magnetic field. In this case, the magnetic field supported deposition will prevent the spiral growth and induce 2D or 3D island growth as shown schematically in Fig. 5(a). At low fields (e.g., 2 T) two-dimensional nuclei are formed, while higher

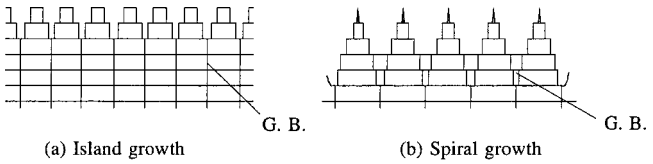

FIG. 5. Schematic illustration of the growth modes of epitaxial thin films grown on silver by CVD in a magnetic field (a) with the magnetic field and (b) without the magnetic field. "G.B." means grain boundary.

magnetic fields lead to three-dimensional nuclei. Thus a highly interconnected film is produced and hence the J_c enhancement.

In contrast, as for the case of absence of the magnetic field, arriving adatoms have enough surface mobility and longer diffusion length at temperatures as high as 850 °C therefore, most of the incoming particles prefer to join into the spirally expanding steps rather than create new nuclei, proposing that those adatoms would follow the spiral growth mode [Fig. 5(b)].

As was demonstrated by Scheel,[17] the growth modes were closely related to the thermodynamic driving forces for epitaxial growth of HTSC films. Different driving forces σ resulted in corresponding different nucleation and growth modes. Under very high driving forces three-dimensional nuclei were formed. A lower but still high σ caused two-dimensional nucleation. The growth spirals become dominant at medium and low σ. The fact also corroborated by the results of Dam *et al.*[18] They found a reproducible transition from spiral growth to 2D nucleation and growth when the background pressure during ablation is increased during pulsed laser deposition (PLD) of YBCO and argued that the change in the kinetic energy of the impinging adatoms is responsible for different growth modes. In addition, Wordenweber *et al.* recently reported that YBCO films deposited via on-axis sputter deposition, which are exposed to a plasma during deposition, also showed 2D nucleation and growth instead of spirals.[19] All this clearly demonstrates that the change from spiral growth to island nucleation and growth can be possible. In other words, at high driving forces many small 2D or 3D nuclei would like to appear. These nuclei obscure the spiral growth and induce the 2D or 3D island growth, which were further confirmed by Monte Carlo simulations of crystal surface initially growing from spiral growth.[20] Clearly, our observation of growth-mode change with magnetic field is in good agreement with this viewpoint.

Since the observation of growth spirals is quite common in YBCO films and screw dislocations are related to these growth features, especially, they are considered to be responsible for the large pinning forces in these materials. The question is now why do we not find growth spirals in our field-assisted deposited films? Where did the screw dislocations go? As we know, spirals form around screw dislocation outcrops. The origin of screw dislocations is explained by substrate defects such as linear or edge defects. It was claimed that such kinds of intrinsic defect structure of the substrate plays a very important role in the nucleation process.[14,21] In contrast to spiral growth, 2D or 3D nucleation

is not related to the occurrence of linear defects; they take place only if the driving force of the system is high enough, and they may occur anywhere on the crystal surface. Hence, under a magnetic field, due to the high driving force, a growth spiral becomes unstable in the case of an increase of the number of island nuclei, leaving 3D nucleation and growth as the dominant growth modes. It should be noted that in order to investigate the dislocation density in the absence of growth spirals, Dam *et al.*[18] have developed a suitable dislocation-specific etching procedure, because dislocation etching is generally the most reliable technique to determine the number of linear defects.[21,22] From their etching experiments they demonstrated that the YBCO films without spiral growth do contain linear defects, but have very low etchpit density (1 per μm^2). We conclude, therefore, that it is not generally clarified that screw dislocations do necessarily form growth spirals. Furthermore, our observation of 2D or 3D nucleation and growth for YBCO films deposited in the presence of a magnetic field implied that other growth mechanisms are possible as well.

CONCLUSIONS

The magnetic field is very effective on yielding superconducting YBCO films on metallic substrates with high critical current densities, but without the use of any buffer layers. Furthermore, we also observe a magnetic-field-induced growth-mode change from spiral growth to island growth in YBCO films. Based on the AFM images, we suggest a growth mechanism to explain the structure of YBCO films grown using the CVD method in a magnetic field. Our model would shed some light on understanding the mechanism of film growth in complex oxides.

ACKNOWLEDGMENTS

One of the authors (Y.M.) is grateful to Dr. H. M. Wang and Y. F. Chen, not only for the great help during the experimental work, but also for many useful discussions. We also thank Y. Hayasaka for the assistance with SEM.

[1] K. Heine, J. Tenbrink, and M. Thoner, Appl. Phys. Lett. **55**, 2441 (1989).
[2] R. D. Ray II and E. E. Hestrom, Physica C **251**, 27 (1995).
[3] Y. Iijima, N. Tanabe, O. Kohno, and Y. Ikeno, Appl. Phys. Lett. **60**, 769 (1992).
[4] D. P. Norton, A. Goyal, J. D. Budai, D. K. Christen, D. M. Kroeger, E. D. Specht, Q. He, B. Saffian, M. Paranthaman, C. E. Klabunde, D. F. Lee, B. C. Sales, and F. A. List, Science **274**, 755 (1996).
[5] T. Aytug, J. Z. Wu, B. W. Kang, D. T. Verebelyi, C. Cantoni, E. D. Specht, A. Goyal, M. Paranthaman, and D. K. Christen, Physica C **340**, 33 (2000).
[6] A. P. Malozemoff, S. Annavarapu, L. Fritzemeier, Q. Li, V. Prunier, M. Rupich, C. Thieme, W. Zhang, A. Goyal, M. Paranthaman, and D. F. Lee, Supercond. Sci. Technol. **13**, 473 (2000).
[7] D. B. Studebaker, J. Zhang, T. J. Marks, Y. Y. Wang, V. Dravid, J. Schindler, and C. Kannewurf, Appl. Phys. Lett. **72**, 1253 (1998).
[8] P. de Rango, M. Lees, P. Lejay, A. Sulpice, R. Tournier, M. Ingold, P. Germi, and M. Pernet, Nature (London) **349**, 770 (1991).
[9] P. J. Ferreira, H. B. Liu, and J. B. Vander Sande, J. Mater. Res. **14**, 2751 (1999).
[10] K. Watanabe, H. Yamane, T. Hirai, N. Kobayoshi, H. Iwasaki, K. Noto, and Y. Muto, Appl. Phys. Lett. **54**, 575 (1989).
[11] K. Watanabe, S. Awaji, J. Sakuraba, K. Watazawa, T. Hasebe, K. Jikihara, Y. Yamada, and M. Ishihara, Cryogenics **36**, 1019 (1996).
[12] Y. Ma, K. Watanabe, S. Awaji, and M. Motokawa, Jpn. J. Appl. Phys., Part 2 **39**, L726 (2000).
[13] Y. Ma, K. Watanabe, S. Awaji, and M. Motokawa, Appl. Phys. Lett. **77**, 3633 (2000).
[14] M. Hawley, I. D. Raistrick, J. G. Beery, and R. J. Houlton, Science **251**, 1587 (1991); D. G. Schlom, D. Anselmetti, J. G. Bednorz, R. F. Broom, A. Catana, T. Frey, Ch. Gerber, H.-J. Güntherodt, H. P. Land, and J. Mannhart, Z. Phys. B: Condens. Matter **86**, 163 (1992).
[15] R. Pinto, P. R. Apte, M. S. R. Rao, R. Chandra, C. P. D'Souza, S. P. Pai, L. C. Gupta, R. Vijayaraghavan, K. I. Gnanasekar, and M. Sharon, Appl. Phys. Lett. **68**, 1006 (1996).
[16] S. Y. Xu, C. K. Ong, and X. Zhang, Solid State Commun. **107**, 273 (1998).
[17] H. J. Scheel, in *Advances in Superconductivity VI*, edited by T. Fuji and Y. Yoiohara (Springer, Tokyo, 1994), p. 29.
[18] B. Dam, N. J. Koeman, J. H. Rector, B. Stäuble-Pümpin, U. Poppe, and R. Griessen, Physica C **261**, 1 (1996).
[19] R. Wordenweber, J. Einfeld, R. Kutzner, A. G. Zaitsev, M. A. Hein, T. Kaiser, and G. Muller, IEEE Trans. Appl. Supercond. **9**, 2486 (1999).
[20] G. H. Gilmer, J. Cryst. Growth **35**, 15 (1976).
[21] D. Eissler, H. S. Wang, and W. Dietsche, Appl. Phys. Lett. **62**, 1292 (1993).
[22] B. Dam, J. M. Huijbregtse, F. C. Klaassen, R. C. F. van der Geest, G. Doornbos, J. H. Rector, A. M. Testa, S. Freisem, J. C. Martinez, B. Stauble-Pumpin, and R. Griessen, Nature (London) **399**, 439 (1999).